doi:10.1016/j.jmb.2010.04.054 J. Mol. Biol. (2010) 399, 637–644

JMB

Available online at www.sciencedirect.com

ScienceDirect

ELSEVIER

Divalent Cations Crosslink Vimentin Intermediate Filament Tail Domains to Regulate Network Mechanics

Yi-Chia Lin[1,2], Chase P. Broedersz[3], Amy C. Rowat[1,2], Tatjana Wedig[4], Harald Herrmann[4], Frederick C. MacKintosh[3] and David A. Weitz[1,2*]

[1]*Department of Physics, Harvard University, Pierce 231, 29 Oxford Street, Cambridge, MA 02138, USA*

[2]*School of Engineering and Applied Sciences, Harvard University, Pierce 231, 29 Oxford Street, Cambridge, MA 02138, USA*

[3]*Department of Physics and Astronomy, Vrije Universiteit, NL-1081 Amsterdam, The Netherlands*

[4]*Division of Molecular Genetics, German Cancer Research Center, D-69120 Heidelberg, Germany*

Received 9 March 2010; received in revised form 24 April 2010; accepted 27 April 2010
Available online 4 May 2010

Edited by R. Craig

Intermediate filament networks in the cytoplasm and nucleus are critical for the mechanical integrity of metazoan cells. However, the mechanism of crosslinking in these networks and the origins of their mechanical properties are not understood. Here, we study the elastic behavior of *in vitro* networks of the intermediate filament protein vimentin. Rheological experiments reveal that vimentin networks stiffen with increasing concentrations of Ca^{2+} and Mg^{2+}, showing that divalent cations act as crosslinkers. We quantitatively describe the elastic response of vimentin networks over five decades of applied stress using a theory that treats the divalent cations as crosslinkers: at low stress, the behavior is entropic in origin, and increasing stress pulls out thermal fluctuations from single filaments, giving rise to a nonlinear response; at high stress, enthalpic stretching of individual filaments significantly modifies the nonlinearity. We investigate the elastic properties of networks formed by a series of protein variants with stepwise tail truncations and find that the last 11 amino acids of the C-terminal tail domain mediate crosslinking by divalent ions. We determined the single-filament persistence length, $l_P \approx 0.5$ μm, and Young's modulus, $Y \approx 9$ MPa; both are consistent with literature values. Our results provide insight into a crosslinking mechanism for vimentin networks and suggest that divalent ions may help regulate the cytoskeletal structure and mechanical properties of cells.

Keywords: cell mechanics; cytoskeleton; rheology

Introduction

Intermediate filaments are highly abundant proteins in the cytoplasm and nucleus of metazoan cells. These proteins form networks[1,2] that are critical for maintaining cell and nuclear shape,[3–7] the mechanical integrity of the cytoplasm,[8] and cell-substrate adhesions.[3] Disruptions in the structure and assembly of intermediate filament networks lead to cell fragility in response to mechanical stress;[1,9] this may furthermore result in destabilization of F-actin and microtubule networks.[3] Moreover, intermediate filaments are implicated in numerous diseases:[10–13] for example, vimentin, the intermediate filament protein, is associated with posterior cataracts[14] and various muscle diseases.[15] To elucidate the structure and assembly of these filaments, purified vimentin provides a tractable, *in vitro* experimental system:[16] These proteins harbor a ~45-nm-long central α-helical "rod" domain, flanked by an amino-terminal "head" domain and a carboxy-terminal "tail" domain, that mediates the formation of parallel coiled-coil dimers,[17] which further associate into antiparallel half-staggered tetramers; these form stable complexes under low-ionic-strength conditions. Upon an increase in the salt concentration to near-physiological values, individual tetramers associate laterally to form ~10-nm-diameter filaments that range in length from a few hundred nanometers to several micrometers.[18] Single-molecule studies reveal that these filaments are highly extensible and elastic;[19–21] thus, intermediate filaments are well-suited to bearing tensional loads under large strains. While single-filament formation and mechanics are better understood, how individual vimentin filaments assemble into cohesive networks and the underlying origin of

*Corresponding author. E-mail address: weitz@seas.harvard.edu.

the mechanical properties of such networks remain poorly understood.

Vimentin networks can also be assembled *in vitro*, allowing the study of their mechanics; these have characteristics of elastic gels,[21,22] which stiffen dramatically with stress.[23] This behavior is similar to that of F-actin networks, which also exhibit the characteristics of an elastic gel that markedly stiffens with stress. However, this behavior requires crosslinking of filaments by proteins, and for actin, more than 80 actin-binding proteins have been identified.[24] By contrast, few crosslinking proteins have been identified for vimentin networks. The only clearly demonstrated method to increase the stiffness of intermediate filament networks is to add divalent cations, such as Mg^{2+}, at millimolar concentrations;[25,26] these concentrations are comparable with those found in several different cell types.[27–29] However, even the origins of this behavior remain unclear. Network stiffness enhanced by divalent cations is thought to involve the highly charged carboxy-terminal tail domain;[25,30] however, the interaction between this domain and divalent ions remains poorly understood at the molecular level. A full understanding of the mechanical properties of vimentin networks thus requires systematic investigation of the roles of both divalent cations and the charged tail group.

Here, we form *in vitro* networks of vimentin proteins and investigate the effect of divalent cations such as Mg^{2+} and Ca^{2+} on both structure and viscoelastic properties. We assemble filaments in the presence of millimolar concentrations of divalent cations and observe no effect on network morphology; however, rheological studies show that network stiffness dramatically increases with divalent cation concentration, suggesting that the cations act as crosslinkers. We model the linear and nonlinear behavior of vimentin networks as an entropic, semiflexible polymer network, similar to that of crosslinked F-actin networks:[31,32] Under small applied stress, the network elasticity is linear and its origin is entropic; increasing stress pulls out thermal fluctuations, resulting in highly nonlinear elasticity. Under even larger applied stress, the extensibility of the individual vimentin filaments themselves contributes an enthalpic component, modifying the nonlinear behavior of the network elasticity. To elucidate the crosslinking interactions, we form vimentin networks using a series of tail-truncated protein variants and show that the last 11 amino acids of the tail domain are crucial in mediating the interaction between vimentin filaments and divalent cations.

Results and Discussion

We investigate the effect of divalent cations on the structure and elastic properties of vimentin networks by incorporating varying concentrations of Mg^{2+} (from 2 to 16 mM) into the polymerization buffer with 1 mg/ml of vimentin; this concentration of protein and Mg^{2+} is comparable with those found in several different cell types.[3,18,27–29] When formed in the absence of any divalent cation, filaments have a smooth surface with a diameter of $\sim 10 \pm 2$ nm, as shown in the transmission electron micrograph of Fig. 1a. Upon adding 4 mM Mg^{2+}, we do not observe any obvious effect on filament morphology or network structure (Fig. 1b). By contrast, divalent cations have a marked effect on network elastic properties. We probe this by measuring the linear viscoelastic moduli: The elastic modulus, G', dominates the viscous modulus, G'' (Fig. 1c), indicating that vimentin networks are predominantly elastic. Since G' is nearly independent of frequency, we characterize the network elasticity by the plateau modulus, G_0. To investigate the effects of both salt concentration and vimentin concentration, c_V, we vary the molar ratios of cations Mg^{2+} and Ca^{2+} to vimentin, R_{Mg} and R_{Ca}, respectively. With the addition of Mg^{2+} at 4 mM for 1 mg/ml of vimentin or $R_{Mg}=215$ (black solid squares), the vimentin networks exhibit markedly higher values of G_0; similar behavior is also observed upon introduction of Ca^{2+} at $R_{Ca}=215$ (solid triangles), as shown in Fig. 1c. To explore the dependence of vimentin network elasticity on R_{Mg}, R_{Ca}, and c_V, we summarize the data for G_0 in a state diagram (Fig. 1d); with variation in the concentration of divalent cations as well as the c_V, the linear elasticity of vimentin networks can be tuned over more than one decade.

To dissect the origins of this tunability, we plot the dependence of G_0 on R_{Mg} for a fixed c_V and find $G_0 \sim R_{Mg}^{0.51}$; a similar scaling behavior is observed for R_{Ca} (Fig. 2a). We also determine how G_0 depends on c_V for a fixed R_{Mg}. In the absence of divalent cations, $G_0 \sim c_V^{1.28}$ (Fig. 2b, open circles), which, within our measurement error, is consistent with $G_0 \sim c_V^{7/5}$, as expected for an entangled solution of semiflexible polymers.[33–35] By contrast, upon addition of Mg^{2+} to $R_{Mg}=134$, the concentration dependence of G_0 increase markedly[26] to $G_0 \sim c_V^{2.13}$; similar behavior is observed for $R_{Mg}=215$, as shown in Fig. 2b. This scaling is in good agreement with that observed for actin networks crosslinked with the rigid crosslinkers scruin[31] and heavy meromyosin;[36] it is also in good agreement with theoretical predictions for crosslinked semiflexible polymer networks.[31,37] Taken together, these findings suggest that divalent cations behave as rigid crosslinkers for vimentin networks.

The mechanical response of networks composed of crosslinked, semiflexible but inextensible polymers can be quantitatively understood in terms of single-filament mechanics, which depends on the persistence length, l_P, or individual filaments, as well as on the spring-like mechanical response of polymer segments on the length scale between crosslinks, l_c; this entropic response is governed by the transverse thermal fluctuations of the polymer segment and is characterized by a spring constant of $90\frac{k_B T l_P^2}{l_c^4}$ in the small strain limit.[37] For a uniform

or affine strain, this leads to a network shear modulus of

$$G_0 = 6\rho \frac{k_B T l_P^2}{l_c^3}, \quad (1)$$

where k_B is Boltzmann's constant, T is the temperature, and ρ is the density of filaments measured by the total length of polymer per unit volume; $\rho = 2.1 \times 10^{13}$ m^{-2} at $c_V = 1$ mg/ml, assuming there is a constant number of 32 molecules per filament cross-section.[38] Thus, in this model, the pronounced variation of G_0 with R_{Mg} is attributed to a change in crosslinking density. Indeed, l_c is directly controlled by R_{Mg}: for a fixed $c_V = 2$ mg/ml, $l_c \sim R^{-0.51/3} \sim R^{-0.17}$.

Additional support for the role of divalent cations as crosslinkers is provided by probing the nonlinear elastic response; this is a hallmark of virtually all crosslinked biopolymer networks.[23] To explore the nonlinearity, we perform a differential stress measurement: We apply constant prestress, σ, while superposing a small-amplitude oscillatory stress, $\delta\sigma(t) = \delta\sigma e^{i\omega t}$, on the network and measure the strain response $\delta\gamma(t)$; this allow us to determine the differential elastic moduli. A creep test confirm that the network response does not change on the timescale of our measurements (SI Fig. 1). For small values of σ, the differential elastic modulus, K', and loss modulus, K'', are identical with G' and G'', respectively. As σ is increased above some critical value, σ_c, K' increases until the network breaks at the maximum prestress, σ_{Max}, and maximum differential modulus, K'_{Max} (Fig. 3a, arrows). Both σ_{Max} and K'_{Max} increase with c_V and R_{Mg}. Remarkably, vimentin networks formed in the presence of Mg^{2+} have 5-fold larger σ_{Max} and K'_{Max} (Fig. 3a, solid symbols). By varying the concentrations of both divalent cations and protein as well as the applied stress, we can tune the nonlinear elastic properties of vimentin networks over more than

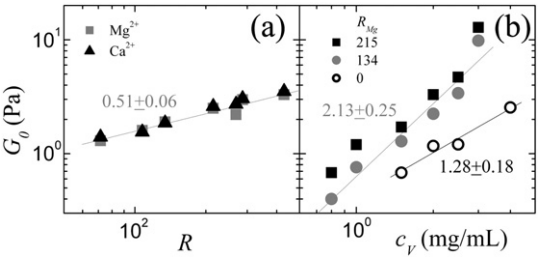

Fig. 2. Dependence of the linear elastic modulus, G_0, on crosslinking density, R, and c_V. (a) In the presence of Mg^{2+} (squares) and Ca^{2+} (triangles), G_0 increases with R, scaling as $G_0 \sim R^{0.51}$ at a fixed $c_V = 2$ mg/ml. (b) In the absence of divalent cations, $G_0 \sim c_V^{1.28}$, while in the presence of divalent cations, the concentration dependence becomes $G_0 \sim c_V^{2.13}$.

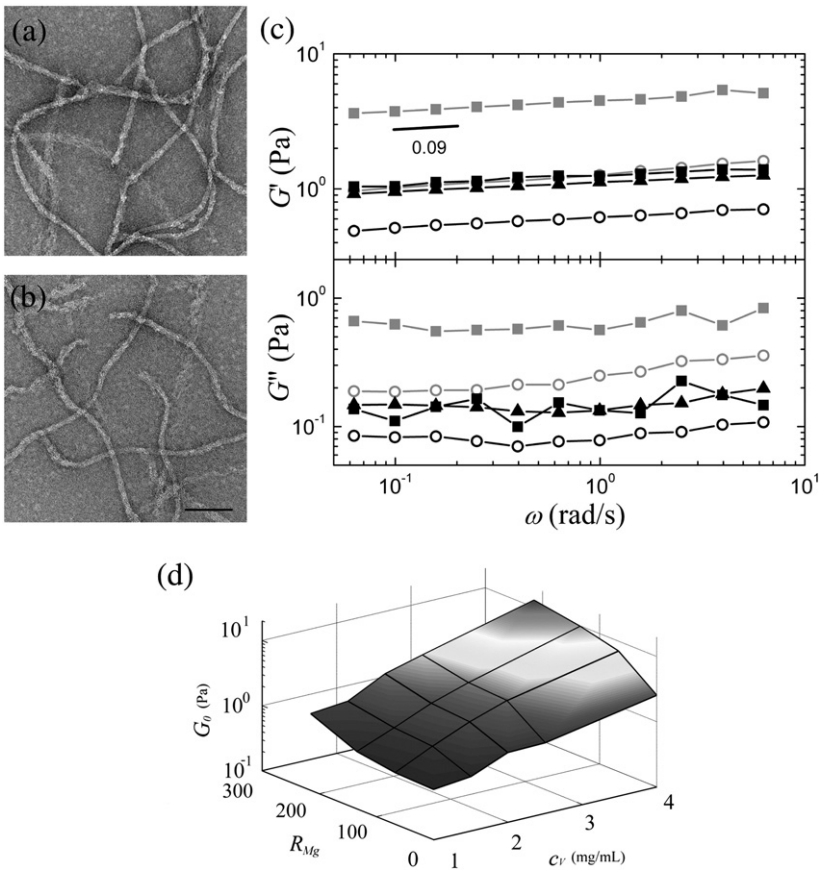

Fig. 1. Effect of divalent cations on the morphology and elasticity of vimentin networks. Transmission electron micrographs of (a) vimentin filaments assembled in the presence of 160 mM Na^+ only and (b) filaments assembled in the presence of 160 mM Na^+ and 4 mM Mg^{2+} ($R_{Mg} = 215$). The scale bar represents 100 nm. (c) Linear viscoelastic shear moduli of vimentin networks in the absence of divalent ions ($c_V = 1$ mg/ml, black open circles; $c_V = 2.5$ mg/ml, gray open circles) and in the presence of Mg^{2+} ($R_{Mg} = 215$; $c_V = 1$ mg/ml, black squares; $c_V = 2.5$ mg/ml, gray squares) and Ca^{2+} ($R_{Ca} = 215$; $c_V = 1$ mg/ml, black triangles). G' dominates over G'' and exhibits weak power-law scaling with frequency, ω, having an exponent of 0.09. The networks in the presence of divalent ions are two to four times stiffer. (d) State diagram summarizing the dependence of the elastic response of vimentin networks on R_{Mg} and c_V.

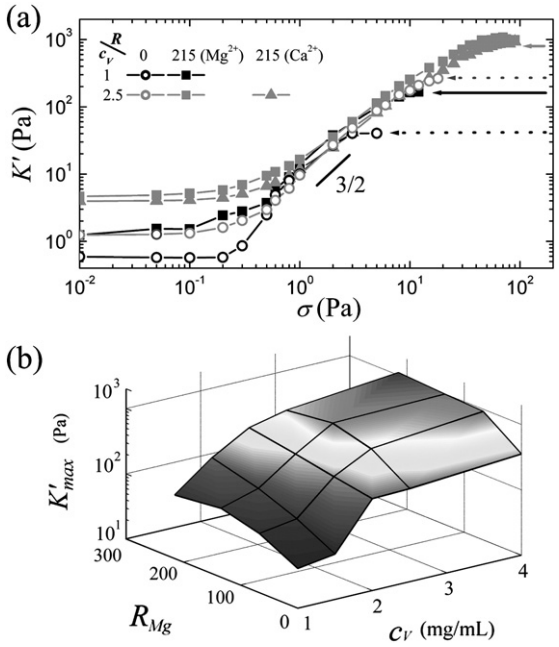

Fig. 3. Nonlinear stress-stiffening behavior of vimentin networks. (a) K' as a function of the applied steady shear stress, σ, for vimentin networks with $R_{Mg}=0$ (open symbols), $R_{Mg}=215$ (solid squares), and $R_{Ca}=215$ (solid triangles). All networks exhibit stiffening when subjected to prestress. Arrows denote the maximum elastic modulus, K'_{Max}. (b) State diagram summarizing dependence of the nonlinear elastic response of vimentin networks on R_{Mg} and c_V.

three decades, as summarized in Fig. 3b. We observe a similar nonlinear response for networks formed in the presence of Ca^{2+} (Fig. 3a), further substantiating that divalent cations act as network crosslinkers.

In the stress-stiffening regime, we observed that $K' \sim \sigma^{3/2}$ over more than one decade, as shown in Fig. 3a. This σ dependence is consistent with the nonlinear elastic behavior predicted by the affine thermal model; this is also observed for permanently crosslinked actin networks.[31] To further probe the mechanism of nonlinear elasticity in vimentin networks, we perform independent least-squares fits of the full theoretical expression[39] to the data for each sample and obtain two fitting parameters: the linear modulus, G_0, and the characteristic stress for the onset of stiffening,

$$\sigma_c = \rho \frac{k_B T l_P}{l_c^2}. \quad (2)$$

With the use of these fitting values to scale the data for networks with varying c_V and R_{Mg}, all the data collapse, as shown in Fig. 4a; this indicates a universal stress-stiffening response. The functional form of the scaled data is in good accord with the theoretical prediction[37,39] for both the linear regime and the nonlinear regime except at the very highest stresses, as shown by the solid gray line in Fig. 4a.

From values of G_0 and σ_c, we determined the value of l_c for each data set, as indicated in Fig. 4a. Moreover, we find a consistent value for l_P (≈0.4–0.5 μm) for all the data sets, which is in accord with previous experiments.[40,41]

At the very highest stresses, $\sigma/\sigma_c > 10$, the experimental data deviate significantly from the theoretical prediction (Fig. 4a). This deviation could result from irreversible network fracture or failure; however, we find that in the high-stress regime just below σ_{Max}, the elastic behavior is fully reversible on the timescales of our measurements (SI Fig. 2). Alternatively, the observed behavior could result from slippage between crosslinks, as can occur in a solution or transiently crosslinked system, such as F-actin solutions without permanent crosslinks;[42] however, such data collapse (Fig. 4a) is not possible when the stiffening exponent varies with protein concentration, as observed for F-actin solutions.[42] Instead, we include the consequences of the extensibility of

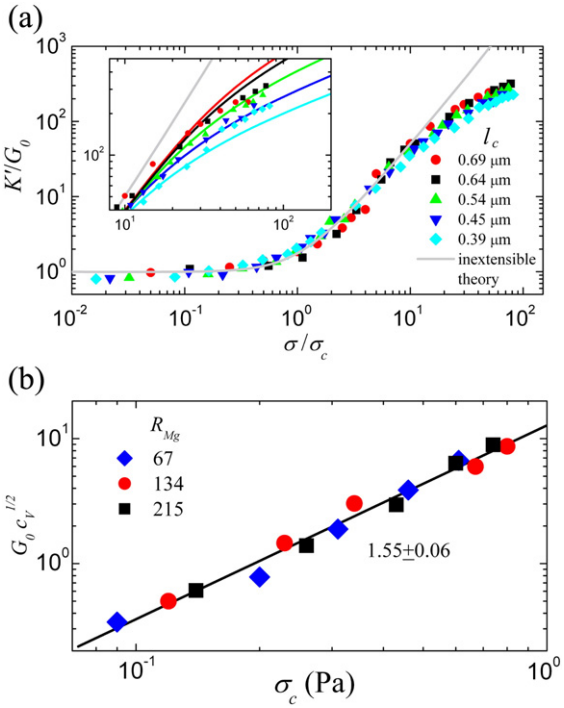

Fig. 4. Elastic response of vimentin networks results from stretching the entropic fluctuations of single semi-flexible filaments at low to intermediate stresses; at high stress, enthalpic stretching of the individual filaments contributes to the nonlinear response. (a) Each data set is rescaled by σ_c and G_0, revealing data collapse that reflects the universal form of the entropic model or inextensible theory (gray line). The departure between the entropic model and our experimental data depends on the l_c: a larger departure is observed at high stress with decreasing l_c. (Inset) Each set of the experimental data (colored symbols) is in agreement with the modified theory (colored lines), which captures the behavior of networks in all stress regimes. (b) Scaling parameters as a function of σ_c for different values of R_{Mg}. The solid line shows a scaling of $\sigma_c^{1.55}$, consistent with the theoretical prediction.

individual filaments. This is motivated by observations that many types of intermediate filaments are highly extensible compared with actin[20,43,44] and appear straightened in human keratinocyte cells subjected to large uniaxial strains of 100%.[43] The extensional modulus depends on intrinsic properties of individual filaments and should thus be independent of l_c, whereas the linear entropic modulus scales as $1/l_c^3$.[37] Thus, network response should be increasingly dominated by the enthalpic stretching mode for smaller values of l_c or for increasing values of σ, where thermal fluctuations are pulled out, thereby increasing the effective spring constant of the entropic mode. Consistent with this, the deviation of the data from the universal curve at high stress increases as l_c decreases, as seen more clearly in the inset of Fig. 4a.

To make a more quantitative comparison, we extend the inextensible, entropic model by introducing an enthalpic stretch modulus, E;[23,45] this parameter describes the resistance of the filament to changes in its contour length and is related to its intrinsic structure and material properties; for a linear elastic rod, E represents the force required to stretch the rod to twice its original length. A value for E can be estimated by assuming the filament behaves as a homogeneous elastic rod of diameter $2r \approx 8$–12 nm, for which $E \approx 4k_BTl_P/r^2 \approx 463$ pN. Interestingly, this is comparable with the force required to unfold coiled-coil domains of vimentin dimers,[46] 200–300 pN. However, at the point where we observe network failure, we estimate that the filaments are stretched to less than twice their length. Moreover, the resulting filament tension is borne by the multiple dimers in cross-section.[38] Thus, these networks break upon application of much lower forces on a per-dimer basis and coiled-coil unfolding is not likely the origin of the network failure. The resulting predictions using this extended theoretical treatment require no further fitting parameters and are in excellent agreement with each set of experimental data for all the strain-stiffening curves, as shown in the inset of Fig. 4a. We also determine Young's modulus to be $Y \approx 9$ MPa, which is consistent with previously reported values of the keratin-like IF proteins from hagfish slime threads.[47,48] Thus, the full nonlinear behavior of vimentin networks is well described by this theory for crosslinked networks of stretchable, semiflexible polymers.

Even more conclusive evidence that these networks are crosslinked is provided by the behaviors of G_0 and σ_c. For a single filament with an l_P at a fixed temperature and polymer concentration, there is one unknown variable, l_c, from Eqs. (1) and (2). To scale out the dependence on l_c, we plot $G_0 c_V^{1/2} \sim G_0 \rho^{1/2}$ *versus* σ_c. This rescaling should result in the collapse of the data for different protein and ion concentrations onto a single curve, which exhibits a 3/2 power law. Indeed, when we plot the σ_c dependence of the quantity $G_0 c_V^{1/2}$, we find a power-law dependence with an exponent of 1.55 ± 0.06, in excellent agreement with this prediction (Fig. 4b).

The divalent cations are clearly playing the role of rigid crosslinkers in these vimentin networks. This is reminiscent of the cation-mediated interactions between neurofilaments, which depend on their anionic carboxy-terminal tail domains;[25] similar effects should also occur for vimentin. We therefore explore the molecular mechanism of this crosslinking by generating a series of stepwise tail-truncated proteins where we delete from 11 to 61 amino acids (Fig. 5a). Although increasing lengths of the tail domain are deleted, the tail-truncated proteins still form gels, which exhibit a network structure similar to the wild-type network (ΔC11, SI Fig. 3b; ΔC36, SI Fig. 3c). Moreover, they show predominantly elastic behavior, with elastic moduli roughly similar to those of the wild-type network in the absence of any divalent cation (Fig. 5b, open bars). By contrast, however, the networks of tail-truncated proteins do not show a significant increase in stiffness upon addition of Mg^{2+} (Fig. 5b, solid bars). Remarkably, even the longest truncated variant lacking only 11 residues, ΔC11, show only negligible stiffening in the presence of Mg^{2+}, suggesting that divalent cations do not effectively crosslink filaments composed of variant proteins with truncated tails. These results suggest that the major putative interaction domain for divalent cations is located within the last 11 residues of the tail domain. The importance of the vimentin tail domain in the ionic crosslinking mechanism is also evident from the nonlinear elastic behavior: neither K'_{Max} nor σ_{Max} is affected by the presence of Mg^{2+} for networks formed from any of the tail-truncated variants (Fig. 5c and d). Analysis of the amino acid composition in this domain reveals four residues that are negatively charged at physiological pH (2× glutamic acid, 2× aspartic acid), making this region more acidic compared with the rest of the tail domain. Moreover, 2 of the last 11 amino acids are histidines, which have a relatively neutral pK_a at physiological pH values; thus, small changes in pH could lead to large changes in crosslinking, thus affecting network mechanical properties. While other charged domains along the filament could also interact with divalent cations and contribute to the strength of interaction among individual dimers within a single filament as well as crosslinking between filaments, the tip of the tail domain clearly has an essential role in mediating network mechanical properties.

Increasing the number of truncation deletions ultimately results in proteins that form filaments with altered morphology, and we observe extensive lateral association of the ΔC61 protein variant (SI Fig. 3d); mechanical measurements reveal these proteins form much weaker networks that cannot sustain the steady stress of the differential measurement and exhibit stress weakening in the nonlinear regime. This variant is truncated in the middle of the evolutionarily conserved intermediate filament consensus motif at the end of the coil 2 domain, indicating that this motif is essential for the structure and mechanical resilience of intermediate filament networks.[49]

Conclusions

The focus of this work is on the role of the carboxy-tail domains in mediating crosslinking interactions among vimentin filaments in networks. Interestingly, interactions among other types of IF proteins may also be mediated by electrostatic interactions between specific protein domains: the charged side arms of neurofilaments are essential for regulating protein–protein interactions,[26] and the higher-order organization of keratin proteins into crosslinked networks is mediated by specific regions of the tail domain,[50] which may ultimately be tuned by salt concentration. Intriguingly, these observations suggest a universality of the mechanisms for tuning the mechanical properties of distinct types of IF networks in their diverse physiological roles.

The results reported in this article highlight the important role of divalent cations in crosslinking vimentin networks. These crosslinks are mediated primarily by the final amino acids in the carboxy-terminal tail domain. The concentrations of divalent cations used in these experiments are comparable with intracellular levels under physiological conditions.[27–29] It is therefore conceivable that divalent cations are also involved in crosslinking intermediate filament networks within cells, thereby providing a mechanism to mediate their mechanical properties. Experiments in living cells are required to address this fascinating issue.

Materials and Methods

Materials

Tail-truncated human vimentin constructs are produced using polymerase chain reaction mutagenesis.[51] Vimentin protein is expressed in *Escherichia coli* (strain TG1) and purified from inclusion bodies as previously described.[52] Purified vimentin protein is stored at −80 °C in 8 M urea, 5 mM Tris–HCl, pH 7.5, 1 mM dithiothreitol (DTT), 1 mM ethylenediaminetetraacetic acid (EDTA), 0.1 mM ethylene glycol bis(β-aminoethyl ether)*N*,*N*′-tetraacetic acid (EGTA), and 10 mM methyl ammonium chloride. On the day before its use, the protein is dialyzed from 8 M urea in a stepwise manner (4, 2, and 1 M urea) into the dialysis

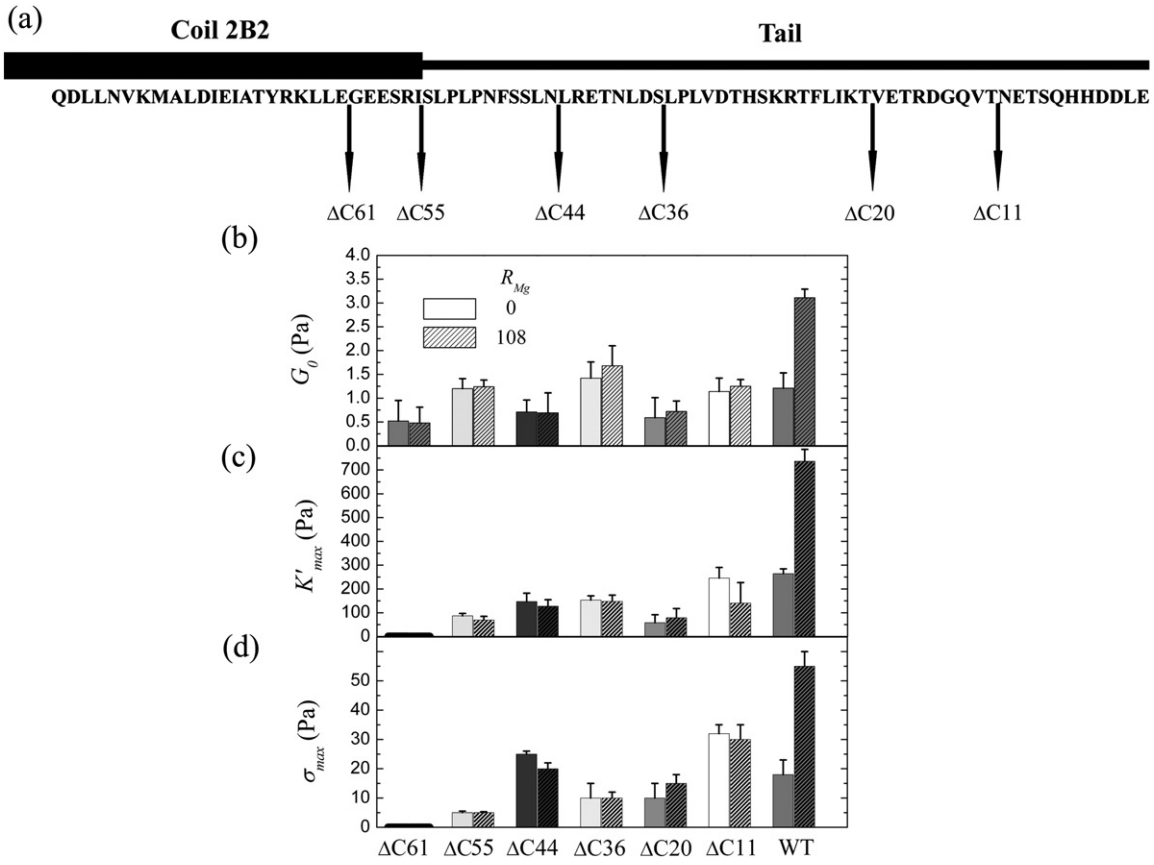

Fig. 5. Linear elastic behavior of vimentin networks formed from a series of stepwise tail-truncated vimentin proteins. (a) Diagram showing the amino acid sequence of six progressively tail-truncated proteins, ΔC11, ΔC20, ΔC36, ΔC44, ΔC55, and ΔC61, and the wild-type protein (WT). (b) Linear elastic shear moduli of vimentin networks with varying tail truncation in the absence of Mg^{2+} (open bars) and in the presence of Mg^{2+} ($R_{Mg}=108$, solid bars) for $c_V=1$ mg/ml. (c and d) Maximum differential elastic modulus, K'_{Max}, (c) and maximum applied steady shear prestress, σ_{Max}, (d) before vimentin networks break in the absence of Mg^{2+} (open bars) and in the presence of Mg^{2+} (2 mM or $R_{Mg}=108$, solid bars). The value of the bar is the mean of three measurements; the error bars represent the standard error.

buffer (5 mM Tris–HCl, pH 8.4, 1 mM EDTA, 0.1 mM EGTA, and 1 mM DTT). After several buffer changes, dialysis is continued overnight at 4 °C against fresh dialysis buffer.[53] The final protein concentration is determined by using a Bradford assay with bovine serum albumin as a standard. To form networks, we add polymerization buffer consisting of 20 mM Tris–HCl, pH 7.0, and 160 mM NaCl, together with 2–16 mM Mg^{2+} ($MgCl^2$) or Ca^{2+} ($CaCl^2$). The sample is polymerized between the rheometer plates for 1 h at 25 °C.

Bulk rheology

Network mechanical response is measured with a stress-controlled rheometer (Gemini HRnano, Malvern Instruments) using a 40 -mm-diameter stainless-steel parallel-plate geometry with a gap size of 120 μm. We use a solvent trap to prevent drying. Linear viscoelastic moduli are obtained by applying oscillatory stress, $\sigma(t) = \sigma e^{i\omega t}$, and measuring the resulting strain, $\gamma(t) = \gamma e^{i\omega t}$. Creep tests are used to study network mechanical behavior on longer timescales: Constant stress is applied for 100 s and then removed; the resultant displacement is measured during creep and subsequent recovery. We measured network behavior in the nonlinear regime with differential measurements. We apply a steady prestress, σ, for 5 s and then superpose a small-amplitude oscillatory stress, $\delta\sigma(t)=\delta\sigma e^{-i\omega t}$; we measure the oscillatory strain response, $\delta\gamma(t)=\delta\gamma e^{-i\omega t}$, at a frequency of $\omega = 0.6$ rad/s. Here, the oscillatory stress is always less than 10% of the steady prestress, and we confirm that the response is linear in δσ for all σ. The complex differential or tangent viscoelastic modulus is given by $K^*(\omega,\sigma) = [\delta\sigma/\delta\gamma]$.

Electron microscopy

Assembled filaments are fixed with an equal volume of 0.2% glutaraldehyde in filament polymerization buffer, applied to glow-discharged carbon-coated copper grids for 15 s, washed with water for 10 s, and stained briefly with uranyl acetate for 15 s. Specimens were examined in a JEOL 2100 transmission electron microscope.

Acknowledgements

This work was supported by the National Science Foundation (DMR-0602684 and CTS-0505929) and the Harvard Materials Research Science and Engineering Center (DMR-0213805). A.C.R. was supported by a Human Frontiers Science Program Cross-Disciplinary Fellowship; H.H., by a grant from the German Research Foundation (DFG HE 1853/4-3). C.P.B. and F.C.M. were supported in part by Foundation for Fundamental Research on Matter/Netherlands Organization for Scientific Research. We thank Julia Jebsen and Eleanor Millman for their expert technical help.

Supplementary Data

Supplementary data associated with this article can be found, in the online version, at doi:10.1016/j.jmb.2010.04.054

References

1. Herrmann, H., Bar, H., Kreplak, L., Strelkov, S. V. & Aebi, U. (2007). Intermediate filaments: from cell architecture to nanomechanics. *Nat. Rev. Mol. Cell Biol.* **8**, 562–573.
2. Lazarides, E. (1980). Intermediate filaments as mechanical integrators of cellular space. *Nature*, **283**, 249–256.
3. Goldman, R. D., Khuon, S., Chou, Y. H., Opal, P. & Steinert, P. M. (1996). The function of intermediate filaments in cell shape and cytoskeletal integrity. *J. Cell Biol.* **134**, 971–983.
4. Lammerding, J., Hsiao, J., Schulze, P. C., Kozlov, S., Stewart, C. L. & Lee, R. T. (2005). Abnormal nuclear shape and impaired mechanotransduction in emerin-deficient cells. *J. Cell Biol.* **170**, 781–791.
5. Goldman, R. D. & Knipe, D. M. (1973). Functions of cytoplasmic fibers in non-muscle cell motility. *Cold Spring Harbor Symp. Quant. Biol.* **37**, 523–534.
6. Gonzales, M., Weksler, B., Tsuruta, D., Goldman, R. D., Yoon, K. J., Hopkinson, S. B. *et al.* (2001). Structure and function of a vimentin-associated matrix adhesion in endothelial cells. *Mol. Biol. Cell*, **12**, 85–100.
7. Tolstonog, G. V., Belichenko-Weitzmann, I. V., Lu, J. P., Hartig, R., Shoeman, R. L., Traub, U. & Traub, P. (2005). Spontaneously immortalized mouse embryo fibroblasts: growth behavior of wild-type and vimentin-deficient cells in relation to mitochondrial structure and activity. *DNA Cell Biol.* **24**, 680–709.
8. Wang, N., Butler, J. P. & Ingber, D. E. (1993). Mechanotransduction across the cell-surface and through the cytoskeleton. *Science*, **260**, 1124–1127.
9. Lane, E. B. & McLean, W. H. I. (2004). Keratins and skin disorders. *J. Pathol.* **204**, 355–366.
10. Beil, M., Micoulet, A., von Wichert, G., Paschke, S., Walther, P., Omary, M. B. *et al.* (2003). Sphingosylphosphorylcholine regulates keratin network architecture and visco-elastic properties of human cancer cells. *Nat. Cell Biol.* **5**, 803–811.
11. Bonifas, J. M., Rothman, A. L. & Epstein, E. H., Jr. (1991). Epidermolysis bullosa simplex: evidence in two families for keratin gene abnormalities. *Science*, **254**, 1202–1205.
12. Herrmann, H., Wedig, T., Porter, R. M., Lane, E. B. & Aebi, U. (2002). Characterization of early assembly intermediates of recombinant human keratins. *J. Struct. Biol.* **137**, 82–96.
13. Parry, D. A. D. & Steinert, P. M. (1995). *Intermediate Filament Structure.* Springer, Austin, TX.
14. Bornheim, R., Muller, M., Reuter, U., Herrmann, H., Bussow, H. & Magin, T. M. (2008). A dominant vimentin mutant upregulates Hsp70 and the activity of the ubiquitin-proteasome system, and causes posterior cataracts in transgenic mice. *J. Cell Sci.* **121**, 3737–3746.
15. Gallanti, A., Prelle, A., Moggio, M., Ciscato, P., Checcarelli, N., Sciacco, M. *et al.* (1992). Desmin and vimentin as markers of regeneration in muscle diseases. *Acta Neuropathol.* **85**, 88–92.
16. Mucke, N., Wedig, T., Burer, A., Marekov, L. N., Steinert, P. M., Langowski, J. *et al.* (2004). Molecular and biophysical characterization of assembly-starter units of human vimentin. *J. Mol. Biol.* **340**, 97–114.
17. Geisler, N. & Weber, K. (1982). The amino acid sequence of chicken muscle desmin provides a common structural model for intermediate filament proteins. *EMBO J.* **1**, 1649–1656.
18. Portet, S., Mucke, N., Kirmse, R., Langowski, J. R., Beil, M. & Herrmann, H. (2009). Vimentin inter-

mediate filament formation: *in vitro* measurement and mathematical modeling of the filament length distribution during assembly. *Langmuir*, **25**, 8817–8823.
19. Guzman, C., Jeney, S., Kreplak, L., Kasas, S., Kulik, A. J., Aebi, U. & Forro, L. (2006). Exploring the mechanical properties of single vimentin intermediate filaments by atomic force microscopy. *J. Mol. Biol.* **360**, 623–630.
20. Kreplak, L., Bar, H., Leterrier, J. F., Herrmann, H. & Aebi, U. (2005). Exploring the mechanical behavior of single intermediate filaments. *J. Mol. Biol.* **354**, 569–577.
21. Yamada, S., Wirtz, D. & Coulombe, P. A. (2003). The mechanical properties of simple epithelial keratins 8 and 18: discriminating between interfacial and bulk elasticities. *J. Struct. Biol.* **143**, 45–55.
22. Janmey, P. A., Euteneuer, U., Traub, P. & Schliwa, M. (1991). Viscoelastic properties of vimentin compared with other filamentous biopolymer networks. *J. Cell Biol.* **113**, 155–160.
23. Storm, C., Pastore, J. J., MacKintosh, F. C., Lubensky, T. C. & Janmey, P. A. (2005). Nonlinear elasticity in biological gels. *Nature*, **435**, 191–194.
24. Dos Remedios, C. G., Chhabra, D., Kekic, M., Dedova, I. V., Tsubakihara, M., Berry, D. A. & Nosworthy, N. J. (2003). Actin binding proteins: regulation of cytoskeletal microfilaments. *Physiol. Rev.* **83**, 433–473.
25. Leterrier, J. F., Kas, J., Hartwig, J., Vegners, R. & Janmey, P. A. (1996). Mechanical effects of neurofilament cross-bridges—modulation by phosphorylation, lipids, and interactions with F-actin. *J. Biol. Chem.* **271**, 15687–15694.
26. Lin, Y.-C., Yao, N. Y., Broedersz, C. P., Herrmann, H., MacKintosh, F. C. & Weitz, D. A. (2010). Origins of elasticity in intermediate filament networks. *Phys. Rev. Lett.* **104**, 058101.
27. Csernoch, L., Bernengo, J. C., Szentesi, P. & Jacquemond, V. (1998). Measurements of intracellular Mg^{2+} concentration in mouse skeletal muscle fibers with the fluorescent indicator Mag-Indo-1. *Biophys. J.* **75**, 957–967.
28. Morelle, B., Salmon, J. M., Vigo, J. & Viallet, P. (1994). Measurement of intracellular magnesium concentration in 3t3 fibroblasts with the fluorescent indicator Mag-Indo-1. *Anal. Biochem.* **218**, 170–176.
29. Polimeni, P. I. (1974). Extracellular space and ionic distribution in rat ventricle. *Am. J. Physiol.* **227**, 676–683.
30. Leterrier, J. F., Langui, D., Probst, A. & Ulrich, J. (1992). A molecular mechanism for the induction of neurofilament bundling by aluminum ions. *J. Neurochem.* **58**, 2060–2070.
31. Gardel, M. L., Shin, J. H., MacKintosh, F. C., Mahadevan, L., Matsudaira, P. & Weitz, D. A. (2004). Elastic behavior of cross-linked and bundled actin networks. *Science*, **304**, 1301–1305.
32. Tharmann, R., Claessens, M. & Bausch, A. R. (2007). Viscoelasticity of isotropically cross-linked actin networks. *Phys. Rev. Lett.* **98**, 088103.
33. Hinner, B., Tempel, M., Sackmann, E., Kroy, K. & Frey, E. (1998). Entanglement, elasticity, and viscous relaxation of actin solutions. *Phys. Rev. Lett.* **81**, 2614.
34. Isambert, H. & Maggs, A. C. (1996). Dynamics and rheology of actin solutions. *Macromolecules*, **29**, 1036–1040.
35. Morse, D. C. (1998). Viscoelasticity of concentrated isotropic solutions of semiflexible polymers: 2. Linear response. *Macromolecules*, **31**, 7044–7067.
36. Luan, Y., Lieleg, O., Wagner, B. & Bausch, A. R. (2008). Micro- and macrorheological properties of isotropically cross-linked actin networks. *Biophys. J.* **94**, 688–693.
37. Mackintosh, F. C., Kas, J. & Janmey, P. A. (1995). Elasticity of semiflexible biopolymer networks. *Phys. Rev. Lett.* **75**, 4425–4428.
38. Steven, A. C., Wall, J., Hainfeld, J. & Steinert, P. M. (1982). Structure of fibroblastic intermediate filaments: analysis of scanning transmission electron microscopy. *Proc. Natl Acad. Sci. USA*, **79**, 3101–3105.
39. Broedersz, C. P., Storm, C. & MacKintosh, F. C. (2009). Effective-medium approach for stiff polymer networks with flexible cross-links. *Phys. Rev. E*, **79**, 061914.
40. Mucke, N., Kreplak, L., Kirmse, R., Wedig, T., Herrmann, H., Aebi, U. & Langowski, J. (2004). Assessing the flexibility of intermediate filaments by atomic force microscopy. *J. Mol. Biol.* **335**, 1241–1250.
41. Schopferer, M., Bar, H., Hochstein, B., Sharma, S., Mucke, N., Herrmann, H. & Willenbacher, N. (2009). Desmin and vimentin intermediate filament networks: their viscoelastic properties investigated by mechanical rheometry. *J. Mol. Biol.* **388**, 133–143.
42. Semmrich, C., Larsen, R. J. & Bausch, A. R. (2008). Nonlinear mechanics of entangled F-actin solutions. *Soft Matter*, **4**, 1675–1680.
43. Fudge, D., Russell, D., Beriault, D., Moore, W., Lane, E. B. & Vogl, A. W. (2008). The intermediate filament network in cultured human keratinocytes is remarkably extensible and resilient. *PLoS ONE*, **3**, e2327.
44. Wagner, O. I., Rammensee, S., Korde, N., Wen, Q., Leterrier, J. F. & Janmey, P. A. (2007). Softness, strength and self-repair in intermediate filament networks. *Exp. Cell Res.* **313**, 2228–2235.
45. Odijk, T. (1995). Stiff chains and filaments under tension. *Macromolecules*, **28**, 7016–7018.
46. Qin, Z., Kreplak, L. & Buehler, M. J. (2009). Hierarchical structure controls nanomechanical properties of vimentin intermediate filaments. *PLoS ONE*, **4**, e7294.
47. Fudge, D. S., Gardner, K. H., Forsyth, V. T., Riekel, C. & Gosline, J. M. (2003). The mechanical properties of hydrated intermediate filaments: insights from hagfish slime threads. *Biophys. J.* **85**, 2015–2027.
48. Schaffeld, M. & Schultess, J. (2006). Genes coding for intermediate filament proteins closely related to the hagfish "thread keratins (TK)" alpha and gamma also exist in lamprey, teleosts and amphibians. *Exp. Cell Res.* **312**, 1447–1462.
49. Herrmann, H., Strelkov, S. V., Feja, B., Rogers, K. R., Brettel, M., Lustig, A. *et al.* (2000). The intermediate filament protein consensus motif of helix 2B: its atomic structure and contribution to assembly. *J. Mol. Biol.* **298**, 817–832.
50. Lee, C. H. & Coulombe, P. A. (2009). Self-organization of keratin intermediate filaments into cross-linked networks. *J. Cell Biol.* **186**, 409–421.
51. Rogers, K. R., Eckelt, A., Nimmrich, V., Janssen, K. P., Schliwa, M., Herrmann, H. & Franke, W. W. (1995). Truncation mutagenesis of the non-alpha-helical carboxyterminal tail domain of vimentin reveals contributions to cellular localization but not to filament assembly. *Eur. J. Cell Biol.* **66**, 136–150.
52. Herrmann, H., Hofmann, I. & Franke, W. W. (1992). Identification of a nonapeptide motif in the vimentin head domain involved in intermediate filament assembly. *J. Mol. Biol.* **223**, 637–650.
53. Herrmann, H., Kreplak, E. & Aebi, U. (2004). Isolation, characterization, and *in vitro* assembly of intermediate filaments. In *Intermediate Filament Cytoskeleton* (Omary, M. B., & Coulombe, P. A., eds) vol. 78, pp. 3–24, Elsevier Academic Press, San Diego, CA and London, UK.